

AlN Contour-Mode Resonators for Narrow-Band Filters above 3 GHz

Matteo Rinaldi, Chiara Zuniga, Chengjie Zuo and Gianluca Piazza

Department of Electrical and Systems Engineering
University of Pennsylvania
Philadelphia, USA

{rinaldim, piazza}@seas.upenn.edu

Abstract— This paper reports on the design and experimental verification of a new class of thin-film (250 nm) Super High Frequency (SHF) laterally-vibrating piezoelectric microelectromechanical (MEMS) resonators suitable for the fabrication of narrow-band MEMS filters operating at frequencies above 3 GHz. The device dimensions have been opportunely scaled both in the lateral and vertical dimensions in order to excite a contour-extensional mode of vibration in nano features of an ultra-thin (250 nm) Aluminum Nitride (AlN) film. In this first demonstration two-port resonators vibrating up to 4.5 GHz were fabricated on the same die and attained electromechanical coupling, k_t^2 , in excess of 1.5 %. These devices were employed to synthesize the highest frequency ever reported MEMS filter (3.7 GHz) based on AlN contour-mode resonator (CMR) technology.

I. INTRODUCTION

In recent years the use of micro and nano electromechanical (MEMS/NEMS) resonators for RF and sensing applications has been extensively explored. The development of compact, low cost and high performance resonators is meant to respond to the growing demand of single-chip and multi-band RF solutions for advanced wireless communication systems. In addition, the scaling of the device dimensions in the nano domain enables the fabrication of ultra-sensitive nanoelectromechanical gravimetric sensors that thanks to their compact form factor and their IC integration capability can be employed, instead of cumbersome and unintegrable quartz crystal microbalance (QCM), for chemical and bio sensing applications.

Different resonator technologies based on electrostatic [1,2] or piezoelectric [3,4] transduction have been investigated. Among these, the Aluminum Nitride (AlN) Contour-Mode resonator (CMR) [3,5] has emerged as one of the most promising in enabling the fabrication of multiple frequency and high performance resonators on the same silicon chip.

High performance AlN CMR devices in the very and ultra high frequency (VHF-UHF) bands with quality factor between 1,000 and 4,000 have been previously demonstrated [5,6].

Nevertheless, the capability of this technology to operate in the super high frequency (SHF) band has not been extensively explored to date. Although one-port NEMS laterally-vibrating AlN resonators based on lateral field excitation (LFE) have been recently demonstrated by our group [7], the unconventional electrode configuration of those devices (bottom electrode not necessary for LFE) prevented us from easily configuring the nano resonators as two-port networks, and hence from fabricating narrow band filters. In this work thickness field excitation (TFE) CMR design is introduced to expand the frequency of operation of this technology in the SHF band to synthesize filters for radar communications or other emerging high frequency wireless standards. The device dimensions have been scaled both in the lateral and vertical directions and a TFE scheme has been employed to excite a higher order contour-extensional mode of vibration in nano-features of an ultra-thin (250 nm) AlN film up to 4.5 GHz. A two-port configuration has been implemented for the resonators presented in here and the highest frequency (3.7 GHz) ever reported filter based on self-coupled AlN CMRs was synthesized [6] by simply electrically cascading two resonator stages.

II. DESIGN

A conventional CMR is composed of an AlN film sandwiched between two metal electrodes. When an AC signal is applied across the thickness (T) of the device a contour-extensional mode of vibration is excited through the equivalent d_{31} piezoelectric coefficient of AlN. Given the equivalent mass density, ρ_{eq} , and Young's modulus, E_{eq} , of the material stack that forms the resonator, the center frequency, f_0 , of this laterally vibrating mechanical structure, is set by the width, W , of the AlN plate and can be expressed as in Eq. (1).

$$f_0 = \frac{1}{2W} \sqrt{\frac{E_{eq}}{\rho_{eq}}} \quad (1)$$

The other two geometrical dimensions, length, L , and thickness, T , can be independently designed to set the

This work was supported by NCMR/NSF grant no. IIS-07-15024, NSF grant no. ECCS-08-22968 and DARPA N/MEMS S&T grant no. HR-001-06-1-0041.

resonator electrical capacitance, C_0 , and its motional resistance, R_m , [3] as expressed in Eq. (2).

$$R_m \propto \frac{T}{L}$$

$$C_0 \propto \frac{LW}{T} \quad (2)$$

In order to scale the resonance frequency, f_0 , above 3 GHz (SHF band), the width, W , needs to be reduced below $\sim 1.2 \mu\text{m}$ (exact value depends upon E_{eq} and ρ_{eq} and therefore the thickness and material properties of the AlN/metal stack). The reduction in width causes a considerable decrease in the device capacitance, C_0 , to the point that its value can fall below the parasitic capacitance of the supporting substrate (silicon in this case). These parasitics negatively affect the electrical response of the device and can completely mask the device output signal. Therefore, scaling of the device resonance frequency into the SHF band needs to be constrained by the need of keeping the value of C_0 above parasitics and simultaneously occupying a small form factor. Specific scaling rules as illustrated in the following section should therefore be followed.

A. Scaling Rules

In order to attain higher frequency of operation, W needs to be made smaller. At the same time, taking into account the constraints on C_0 , the surface area of the CMR needs to be increased and its thickness reduced (Eq. 2). For this purpose the following criteria need to be followed:

- Mechanically couple a large number, n , of sub-resonators whose width, W , has been scaled to operate in the SHF band (Fig. 1b). In this way a higher order mode of vibration is excited in the AlN plate (f_0 is set by W) but the capacitance of the device is n times larger (total width equal to $n \cdot W$).
- Reduce the thickness, T , of the AlN film (Fig. 1c). This is extremely important in order to further increase the device capacitance while simultaneously keeping small the effective area occupied by the device.
- Reduce the length, L , of the resonator (Fig. 1d) in order to avoid loading the quality factor of the device with the electrical resistance of the metal electrodes. The reduction in the length of the electrode compensates for the increase in resistance associated with the scaling of the electrode width.

The devices presented in this work were designed in accordance to these design rules in order to operate at frequencies above 3 GHz. A two-port configuration was chosen, since it enables the synthesis of narrow-band filters by simply electrically cascading two resonator stages.

B. SHF two-port AlN CMR design

The SHF two-port AlN CMR resonator (Fig. 2) consists of an ultra-thin (250 nm) AlN film sandwiched between a bottom Pt (50 nm) and a top Au (100 nm) electrodes. The

bottom Pt is a single electrode connected to electrical ground, while the top Au layer (chosen for its very low resistivity) is patterned in n parallel electrodes whose width varies between 0.4 and $0.7 \mu\text{m}$ depending upon the desired frequency of operation.

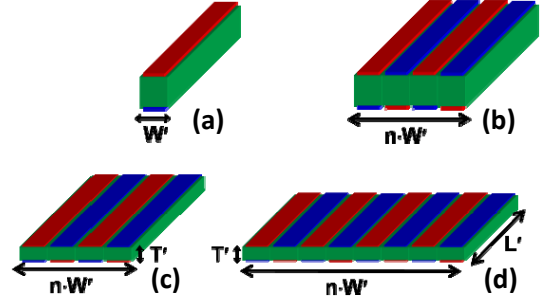


Figure 1. Schematic representation of the CMR scaling to SHF: (a) scaling of the width to increase the frequency; (b) mechanical coupling of a large number of scaled sub-resonators to increase the device capacitance; (c) reduction of the AlN film thickness to increase capacitance and reduce device form factor; (d) reduction of the device length to compensate for increase in electrode resistance due to scaling of the width.

A number n_{in} of the top Au electrodes are connected to form the input port and the remaining (n_{out}) are used to form the output port. The frequency setting width, W , of the sub-resonators forming the electromechanical structure was varied between 0.7 and $1.2 \mu\text{m}$ in order to achieve resonance frequencies between 3 and 4.5 GHz. The number, n , of mechanically coupled sub-resonators was varied between 37 and 67 and the device length, L , was fixed to $17 \mu\text{m}$.

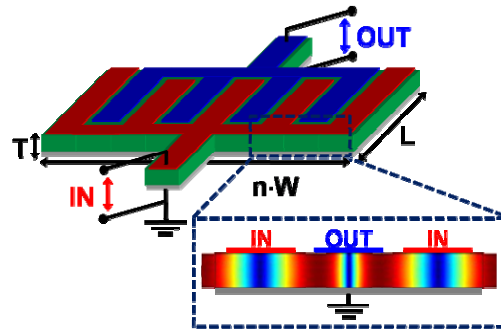


Figure 2. Schematic representation of the designed SHF two-port CMR. The inset shows a 2D FEM simulation of the device mode of vibration: when an AC signal is applied to the input port, the electric field across the thickness of the AlN causes an in plane deformation of the structure through the equivalent d_{31} piezoelectric coefficient and excites the resonator in a contour-extensional mode of vibration. Because of the direct piezoelectric effect, charge is generated and collected by the sensing electrodes (output port).

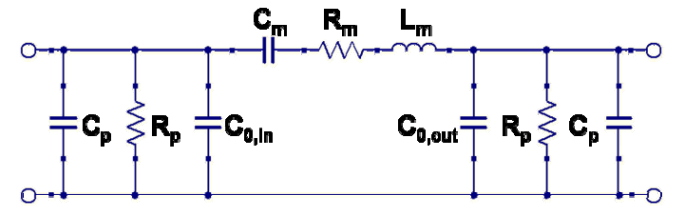


Figure 3. Equivalent electrical circuit for the two-port AlN CMR. C_p and R_p are parasitic components due to the substrate.

The equivalent electrical model of the two-port AlN CMR is shown in Figure 3. All the equivalent electrical parameters

can be expressed as a function of the resonator capacitance, C_o , the frequency of operation, ω_o , the electromechanical coupling, k_t^2 , and quality factor, Q [8].

C. SHF narrow-band CMR filter design

The configuration of the CMR device as a two-port network enabled the direct synthesis of the first prototype of SHF filters based on CMR technology. For this purpose, two resonator stages were electrically cascaded in series to form narrow band filters operating up to 3.7 GHz.

The coupling technique is based on the use of the intrinsic capacitance of a two-port device and permits the definition of band pass filters by simply employing same frequency resonators [6]. This is different from conventional ladder configurations [9], which require two different frequency devices and have an associated negative impact on filter yields.

The equivalent electrical model of the second order filter based on self-coupled AlN CMRs is shown in figure 4.

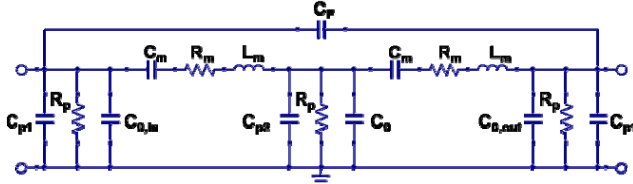


Figure 4. Equivalent electrical circuit for the second order filter based on self-coupled AlN CMRs. C_{p1} , C_{p2} , and R_p are the parasitic component that shunt the input and output ports of the device. C_r is the parasitic feed-through capacitance between input and output ports.

It is important to note that the presence of parasitic capacitances in parallel to the input and output ports of the device reduces the effective electromechanical coupling coefficient, $k_{t,eff}^2$, of the resonators (3).

$$k_{t,eff}^2 = \frac{\pi^2}{2} \frac{C_m}{C_o + C_p} \quad (3)$$

Consequently, the bandwidth of the filter is reduced (since it is directly proportional to $k_{t,eff}^2$) and its insertion loss deteriorated [6]. These points further justify the necessity to maintain the value of the device capacitance, C_o , well above the parasitics when scaling the device to higher frequencies of operation.

III. FABRICATION PROCESS

The devices presented in this work were fabricated combining optical and electron-beam lithography techniques. A 4 mask post-CMOS compatible fabrication process was employed (Fig. 5).

The platinum (Pt) bottom electrode was first patterned by lift-off on top of a high resistivity silicon wafer. The ultra-thin (250 nm) AlN film was sputtered deposited and its quality was optimized to achieve rocking curve values as good as 2.1° (equivalent to what has been obtained in micron-size devices). The optimization was conducted in collaboration with Tegal Corporation. Vias to the bottom electrode pads were opened in

the thin AlN film by wet etching in phosphoric acid (H_3PO_4). Optical lithography was performed for the definition of both the top electrode contact pads and the alignment marks for the subsequent electron-beam lithography step. The in-plane dimensions of the resonators were defined by dry etching of the ultra-thin AlN film in Cl_2 -based chemistry using photoresist as a mask. The top gold electrode pattern was defined by electron-beam lithography and lift-off. Finally, the device was released from the silicon substrate by isotropic dry etching in XeF_2 .

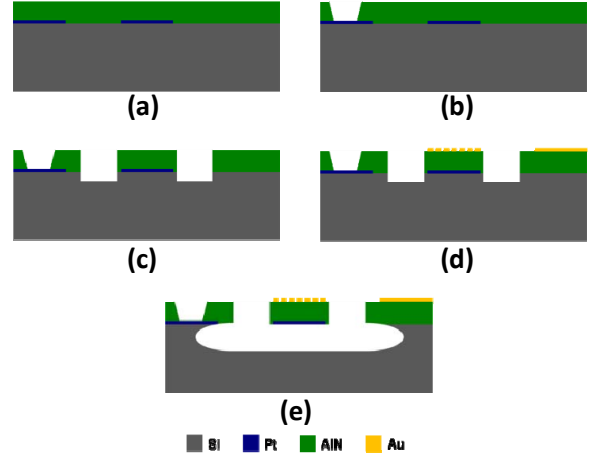


Figure 5. 4 mask post-CMOS compatible fabrication process: (a) sputter deposition of Pt on high resistivity Si substrate and sputterdeposition of the ultra-thin (250 nm) AlN film; (b) open vias in AlN to access bottom electrode; (c) dry etching of AlN in Cl_2 based chemistry; (d) patterning of top Au electrode by electron-beam lithography and lift-off; (e). XeF_2 dry release of the AlN resonator.

It is worth noting that, although electron-beam lithography was employed, the minimum features (400 nm) can also be defined by state-of-the-art optical lithography used in CMOS foundries.

The SEM pictures of a fabricated 3.5 GHz device is shown in figure 6.

IV. EXPERIMENTAL RESULTS AND DISCUSSION

The fabricated devices were tested in an RF probe station and the scattering parameters were measured by an Agilent® N5230A Network Analyzer after performing a short-open-load-through (SOLT) calibration on a reference substrate.

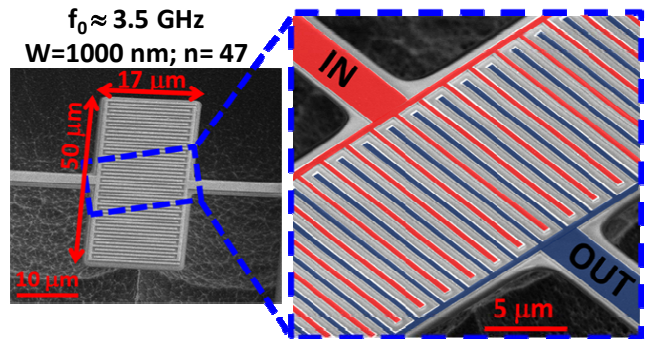


Figure 6. SEM picture of the fabricated 3.5 GHz two-port CMR.

A. SHF two-port CMRs

The measured electrical responses of the SHF two-port CMRs were fitted to the equivalent electrical circuit in Figure 3 and both the experimental and fitted curves of a 3.5 GHz device are shown in Figure 7. The values of the parasitic components, C_p and R_p , were measured by means of de-embedding structures fabricated on the same silicon chip. The quality factor, Q , and the intrinsic electromechanical coupling, k_t^2 , of the resonator were obtained from the fitted curves.

It is important to note that an fQ product as high as $1.7 \cdot 10^{12}$ Hz was measured. This value is approximately one order of magnitude greater than the one measured for lower frequency two-port CMRs [6]. In addition a value of k_t^2 at least 5 times higher than the one reported by the same group for SHF lateral filed excited (LFE) NEMS resonators [7] has been measured. The higher k_t^2 enables the synthesis of narrow-band SHF filters.

A list of the fabricated CMRs operating above 3 GHz along with the corresponding geometrical dimensions and values of k_t^2 and Q is reported in Table I.

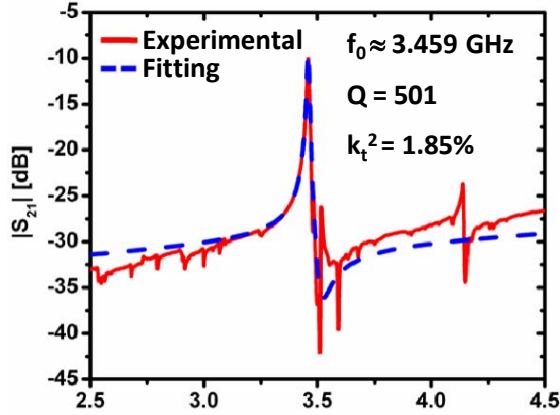


Figure 7. Experimental response and equivalent model fitting for the fabricated 3.5 GHz two-port CMRs.

B. SHF second order filters based on AlN CMRs

The measured electrical responses of the fabricated SHF narrow-band filters are shown in Figure 8. The data was fitted with the equivalent electrical circuit shown in Figure 4 and the values of parasitic components were measured by means of on-chip integrated de-embedding structures.

TABLE I. DIMENSIONS AND EXTRACTED PARAMETER OF FABRICATED CMRS

Frequency of Operation	k_t^2	Q	$n \cdot W$ [μm]	L [μm]
3.04 GHz	1.5%	520	37x1.2	17
3.46 GHz	1.85%	500	47x1	17
4.54 GHz	1.3%	360	67x0.7	17

In these filters, the measured values of the device geometrical capacitance and parasitics are comparable. This,

as explained in Section II, greatly reduces the effective electrometrical coupling of the resonators, therefore limiting the filter bandwidth and deteriorating its insertion loss. In order to simulate the de-embedded response of the filter, the measured parasitic capacitance, C_p , was removed from the equivalent circuit of the filter. In Figure 9 the de-embedded response of the 3 GHz filter is plotted for different values of quality factor, Q , and compared to the one that includes parasitics.

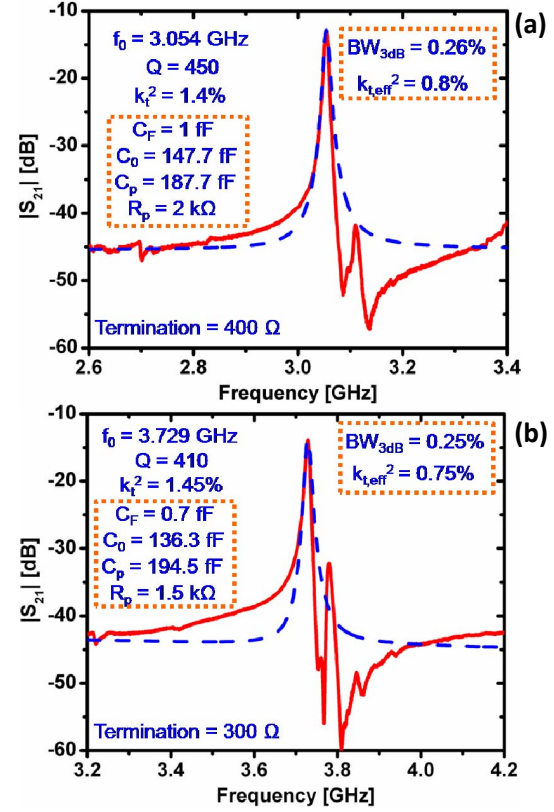


Figure 8. Experimental response and equivalent model fitting of the fabricated 3 GHz (a) and 3.7 GHz (b) second order filters based on two self-coupled CMRs. Q and k_t^2 values refer to the individual resonators forming the filter.

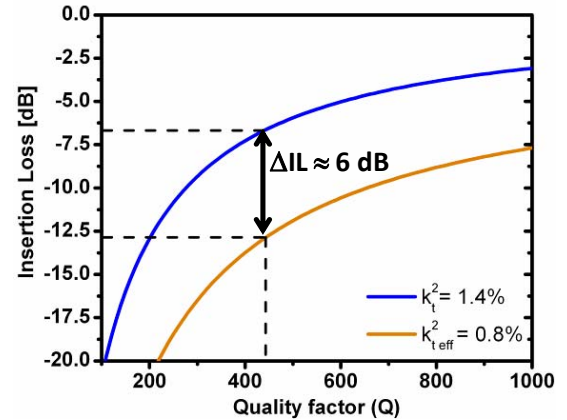


Figure 9. De-embedded ($k_t^2=1.4\%$) and as-fabricated ($k_{t,eff}^2=0.8\%$) insertion loss of the 3 GHz filter plotted for different values of quality factor, Q .

For the actual measured value of Q (450) an improvement in insertion loss of approximately 6 dB is observed in the de-

embedded response. At the same time, if the parasitic effects were to be removed, the filter bandwidth would increase up to the value set by the intrinsic electromechanical coupling of the fabricated CMRs. The improved value of insertion loss (~ 6.5 dB) and wider bandwidth could be attained on the same silicon substrate by simply making the device capacitance, C_0 , even larger and well above the parasitic components. Additionally, the parasitics can be further reduced by optimizing the configuration of the test pads.

These devices represent the first prototype of SHF filters based on AlN CMRs. The filters' performance can be improved to a large extent by optimizing the resonator in-plane geometry so as to increase the transducer capacitance and by acting on the figure of merit, $k_t^2 \cdot Q$, of the device.

V. CONCLUSION

In this paper the design, fabrication and testing of two-port AlN Contour-Mode resonators operating in the SHF band up to 4.5 GHz have been demonstrated. Design issues and scaling rules necessary to operate AlN CMRs above 3 GHz have been introduced and discussed. An ultra-thin (250 nm) AlN film has been employed to fabricate SHF resonators with values of k_t^2 in excess of 1.5 % and $f \cdot Q$ product as high as $1.7 \cdot 10^{12}$ Hz. The capability of these devices to be employed for the fabrication of narrow band filters has been proven by the synthesis of the highest frequency (3.7 GHz) 2nd order filter based on electrically self-coupled AlN contour-mode devices. The importance of the $k_t^2 \cdot Q$ product on the filter performance (insertion loss and bandwidth) has been analyzed and the effect of parasitic components on the response of the SHF filters has also been modeled. The demonstrated features and the disclosed

potentialities of the SHF-scaled CMR devices suggest that this is an excellent candidate for the implementation of compact, low power and high performance RF components for radar communications and other SHF wireless applications.

ACKNOWLEDGMENT

The authors wish to thank the staff of the Wolf Nanofabrication Facility (WNF) at The University of Pennsylvania and Tegal Corporation for their help with the deposition of thin AlN films.

REFERENCES

- [1] K. Wang, A.-C. Wong and C. T.-C. Nguyen, *J. Microelectromech. Syst.*, vol. 9, no. 3, pp. 347-360, 2000.
- [2] D. Weinstein, S. A. Bhave, *Proceedings IEEE International Electron Devices Meeting '07*, pp. 415-418, 2007.
- [3] G. Piazza, P.J. Stephanou, A.P. Pisano, *J. Microelectromech. Syst.*, vol. 15, no.6, pp. 1406-1418, 2006.
- [4] R. Abdolvand, G.K. Ho, J. Butler, F. Ayazi, *Proceedings IEEE Micro Electro Mechanical Systems (MEMS), 2007*, pp.795-798, 21-25 Jan. 2007
- [5] P. J. Stephanou, J. P. Black, A. L. Benjamin, *Proceedings IEEE Radio Frequency Integrated Circuits Symposium '08*, pp. 171-174, 2008.
- [6] C. Zuo, N. Sinha, M. B. Pisani, C. R. Perez, R. Mahameed, G. Piazza, *Proceedings IEEE Ultrasonics Symposium '07*, pp. 1156-1159, 2007.
- [7] M. Rinaldi, C. Zuniga, G. Piazza, *Proceedings IEEE MEMS'09 Conference*, pp. 916-919, 2009.
- [8] M. Rinaldi, C. Zuniga, C. Zuo, G. Piazza, *Proceedings 15th International Conference on Solid-State Sensors, Actuators and Microsystems*, pp. 577-580, June 21 - 25, 2009.
- [9] G. Piazza, P. J. Stephanou, A. P. Pisano, *J. Microelectromech. Syst.*, vol. 16, no.2, pp. 319-328, 2007.